Respiration Physiology, **80** (1990) 279–298
Elsevier

RESP 01651

Control of ventilation in the hypercapnic skate *Raja ocellata*: II. Cerebrospinal fluid and intracellular pH in the brain and other tissues

C.M. Wood[1], J.D. Turner[2], R.S. Munger[1] and M.S. Graham[3]

[1] *Department of Biology, McMaster University, Hamilton, Ontario, Canada,* [2] *Department of Animal Science, Macdonald College, McGill University, Ste. Anne de Bellevue, P.Q., Canada and* [3] *Vancouver Public Aquarium, Vancouver, B.C., Canada*

(Accepted 24 February 1990)

Abstract. This study examined the possible role(s) of central acid–base stimuli in the increase in ventilation induced by hypercapnia in the skate, a response that is not due to an O_2 signal (Graham *et al.*, *Respir. Physiol.*, 1990, 80: 251–270). Skate were sampled for cerebrospinal fluid (CSF) acid–base status, intracellular pH of the brain (^{14}C-DMO method), and pHi in other tissues throughout 24 h of exposure to $P_{I_{CO_2}}$ = 7.5 Torr. CSF P_{CO_2} rapidly equilibrated with the elevated $P_{a_{CO_2}}$. Despite the much lower non-HCO_3^- buffer capacity in the CSF, CSF pH was not depressed to the same extent as blood pHa. CSF pH was also regulated more rapidly, returning to control levels by 8–10 h, whereas pHa remained significantly depressed at 24 h. Similarly, the pHis of the weakly buffered brain and heart ventricle were initially compensated more rapidly than those of more strongly buffered white muscle and red blood cells. However, brain pHi adjustment slowed markedly after 4 h and stabilized at only 70% compensation by 20–24 h, suggesting that brain intracellular acidosis may play a role in the long-term increase in ventilation. CSF and brain were the only compartments which did not exhibit an apparent compounding metabolic acidosis during the initial stages of hypercapnic exposure. While these results illustrate the primacy of central acid–base regulation, they do not support a role for CSF pH in the long-term elevation of ventilation in response to hypercapnia. Depressions in pHa and brain pHi appear the two most likely candidates for proximate stimuli.

Animal, skate; pH, cerebrospinal fluid of skate; Buffering, skate tissue; Cerebrospinal fluid, acid–base balance; Control of breathing, cerebrospinal fluid of skate, response to CO_2; Hypercapnia, ventilatory response of skate; pH, intracellular; Technique in respiratory physiology, DMO; Ventilation, sensitivity to CO_2 in skate

In the preceding paper (Graham *et al.*, 1990), we have shown that environmental hypercapnia induces a pronounced and persistent increase in ventilation in the Atlantic

Correspondence to: C.M. Wood, Department of Biology, McMaster University, Hamilton, Ontario, Canada L8S 4K1.

big skate (*Raja ocellata*). As blood and environmental O_2 levels were maintained constant, the response was not due to a disturbance of the primary O_2 drive on ventilation. Rather, it appeared to reflect a direct influence of some aspect of internal acid–base status, acting as an important secondary control on ventilation. Of the parameters measured, depression of arterial blood pHa, rather than elevation of arterial Pa_{CO_2}, appeared to be the most likely candidate for the proximate stimulus. Heisler *et al.* (1988) and Heisler (1989) reached a similar conclusion based on their analysis of ventilatory adjustments during hyperoxia in the larger-spotted dogfish (*Scyliorhinus stellaris*).

These findings suggest that water-breathing fish may already possess the ventilatory sensitivity to acid–base status characteristic of air-breathing vertebrates. However, it is not at all clear that the mechanism is the same. For example, in mammals, the primary CO_2 drive on ventilation is mediated mainly through the central chemoreceptive area in the medulla, with additional input from peripheral chemoreceptors in major arteries (O'Regan and Majcherczyk, 1982; Cherniack *et al.*, 1988). Only the latter appear to be directly sensitive to pHa. For the central chemoreceptors, Pa_{CO_2}, rather than pHa, is the important variable, but CO_2 exerts its effects by crossing the blood–brain barrier and lowering pH in the brain fluids. The proximate stimulus is thought to be the decrease in cerebrospinal fluid (CSF) pH, medullary interstitial pH, medullary intracellular pH (pHi), or some combination thereof (see papers in Schlaefke *et al.*, 1983; Cherniack *et al.*, 1988).

There is very little information available on central acid–base status in fish, and almost none on its relationship with ventilation. The one important exception is the classic work of Maren (1962a,b; 1972) on CSF acid–base regulation in the spiny dogfish (*Squalus acanthias*). Maren demonstrated that CO_2 rapidly penetrated into the CSF from the arterial blood, and that CSF pH was almost perfectly regulated in the face of systemic respiratory acidosis induced by environmental hypercapnia. He speculated that this highly efficient regulation of CSF pH was critical to respiratory control, though without any direct evidence. Measurements of ventilation during hypercapnia in *S. stellaris* by Randall *et al.* (1976) supported this idea, because disturbance of ventilation was shortlived (<2 h), while the disturbance of pHa was prolonged.

In light of this complex situation, the present study was designed to monitor CSF acid-base status, brain pHi, and their relationships with arterial blood status in *R. ocellata* during a hypercapnic regime identical to that of the preceding paper (Graham *et al.*, 1990). Thus the various parameters could be compared directly with the measured ventilatory changes. An additional goal was to compare the time course of pHi adjustment in the brain with that in other tissues (red blood cells, heart ventricle, white muscle) during hypercapnia. Previous studies on other forms of acid–base disturbance (*e.g.* temperature change, exercise) have indicated considerable heterogeneity between tissue compartments in the rate and extent of pHi regulation (Milligan and Wood, 1986; Heisler, 1989).

Materials and methods

Experimental animals and regime. Specimens of the big skate (*Raja ocellata* Mitchill; 0.75–5.0 kg) were caught, held, and fitted with arterial and extradural fluid (EDF) catheters as described by Graham *et al.* (1990). The animals were allowed to recover in darkened, individual experimental chambers served with flowing seawater (salinity = 30 ± 1 ppt) at 12 ± 1 °C for 24–72 h prior to experimentation. *In vivo* measurements were taken from a total of 40 animals, while an additional 10 skate provided fluids and tissues for *in vitro* buffer capacity measurements.

The exposure to hypercapnia was designed to duplicate that employed in the companion study (Graham *et al.*, 1990). However, each animal was sampled only once, rather than repetitively, for measurements of acid–base status in the cerebrospinal (CSF) and extradural (EDF) fluids, and intracellular pH in the brain and other tissues. Groups of skate were sampled under control conditions (PI_{CO_2} = 0.3 Torr, PI_{O_2} = 155 Torr) (N = 9) and under normoxic hypercapnia (PI_{CO_2} = 7.5 Torr, PI_{O_2} = 155 Torr) at 0.5 h (N = 5), 2 h (N = 6), 4 h (N = 6), 8–10 h (N = 5), and 20–24 h (N = 9) of exposure.

Intracellular pH determinations. Intracellular pH (pHi) in brain, heart ventricle, and white muscle was measured using the DMO technique (5,5-dimethyl-2,4-oxazolidinedione) technique originated by Waddell and Butler (1959), with mannitol as the extracellular fluid volume marker. The method used in the present study has been described in detail and critically evaluated previously (Milligan and Wood, 1986, 1987; Wright *et al.*, 1988). Once the DMO has initially equilibrated in a tissue compartment, its redistribution in response to a pH change occurs quickly; Milligan and Wood (1985) have demonstrated that this method reliably measures rapid changes (≤ 15 min) in pHi in fish tissues. In brief, skate were injected, via the arterial catheter, with a 1 ml/kg dose of 7 μCi/ml ^{14}C-DMO (New England Nuclear; specific activity 50.0 mCi/mmol) plus 28 μCi/ml ^{3}H-mannitol (New England Nuclear; specific activity 27.4 mCi/mmol) in 300 mmol/L NaCl, followed by an equal volume of skate saline (composition as described by Graham *et al.*, 1990). The injection was administered 10–12 h prior to the planned time of sacrifice (see above). Tissue intracellular pHi, extracellular fluid volume (ECFV), and intracellular fluid volume (ICFV) were calculated from measurements of extracellular pH (pHa), plasma and tissue water contents, and plasma and tissue ^{14}C-DMO and ^{3}H-mannitol radioactivities, using the equations given by Wright *et al.* (1988). The pK of DMO at experimental temperature was interpolated from the measurements of Heisler *et al.* (1976) at comparable ionic strength.

Sampling protocol. Immediately prior to sacrifice, inspired water, EDF, and arterial blood samples were drawn into gas-tight glass syringes. Water samples were analyzed for PI_{CO_2} and PI_{O_2}, EDF samples (1.0 ml) for pH, C_{CO_2}, protein, Na^+, K^+, Ca^{2+}, Cl^-, ^{14}C-DMO and ^{3}H-mannitol radioactivities, and blood samples (2.1 ml) for Pa_{CO_2}, Pa_{O_2}, true plasma Ca_{CO_2}, whole blood pHa, red cell lysate pH (RBC pHi), hematocrit

(Hct), hemoglobin (Hb), total nucleoside triphosphates (NTP), and plasma protein, Na^+, K^+, Ca^{2+}, Cl^-, and ^{14}C-DMO and ^3H-mannitol radioactivities.

Within 3 min of blood sampling, the animal was removed from the water, and the CSF sampled within a further 2 min. The animal was then quickly killed by excision of the brain; a Dremel Moto-Tool saw (Emerson Electronics, Racine, Wisconsin) was used to rapidly cut the overlying chondocranial cartilage. In our experience, CSF could be obtained only if the extradural fluid was left in place and the spinal cord was not sectioned, preventing hydrostatic collapse of the brain. Anaerobic CSF samples were drawn using a specially modified 100 μl gas-tight glass syringe (Hamilton, Reno, Nevada). The syringe needle was cut off at a length of 2 cm, bevelled at the end, and fitted with a cuff to limit the depth of penetration. The needle was inserted into either the third ventricle of the brainstem (through the transparent paraphysis, a small pouch immediately anterior to the optic lobes) or the fourth ventricle (through the cerebellum). The two ventricles are contiguous. CSF samples were drawn into the syringe using very gentle suction to minimize CO_2 loss from this poorly buffered fluid (*cf.* Weiskopf *et al.*, 1977), and then immediately injected (rather than drawn) into a Radiometer G97-G2 capillary microelectrode. The pH electrode was preconditioned to the same ionic strength with skate saline. The volume of CSF obtained from individual skate varied from 15 to 200 μl, and averaged about 50 μl. After measurement of CSF pH, the polyethylene KCl bridge was then cut off to minimize contamination. The sample was then retrieved from the electrode by gentle suction and analyzed for ^{14}C- and ^3H-radioactivities, protein, and C_{CO_2}, with the latter taking priority in cases of limited sample volume.

Samples of brain (from the medulla oblongata to the olfactory lobes inclusive), heart ventricle, and white muscle (from the epaxial muscle forming the dorsal surface of the "wings") were excised. The tissues were briefly rinsed in skate saline to remove external EDF or blood, and then thoroughly blotted, prior to subdivision and weighing for water content and ^{14}C- and ^3H-radioactivity measurements.

Buffer capacity determinations. The non-HCO_3^- buffer capacities (β_{NB}) of CSF, EDF, and separated blood plasma from 3 skates were determined at 12 °C by tonometry, as described by Graham *et al.* (1990). Buffer capacities of brain, white muscle, heart ventricle, and packed red cells were determined from 5–6 animals for each tissue. Acid titration of tissue homogenates was employed, as described by Cameron and Kormanik (1982), using a Corning 476051 pH electrode. This technique measures total physicochemical buffer capacity (*i.e.* non-HCO_3^- plus HCO_3^- buffering). However, as the original HCO_3^- content of the tissues is low and the P_{CO_2} is kept close to zero during titration, the contribution of the HCO_3^- component is neglible; in essence the results yield an estimate of non-HCO_3^- β.

Brain, white muscle, and heart ventricle were prepared as described above; packed red cells were obtained by centrifugation of whole blood at 9000 × *g* for 2 min followed by removal of plasma by aspiration. Approximately 1/3 of each sample was dried to a constant weight at 65 °C for original water content. The other 2/3 were frozen on dry

ice and pulverized with a mortar and pestle. As a slight hydration occurred during pulverization, half of this powder was dried to a constant weight to find the post-pulverization water content. The other half (0.5–1.0 g) was suspended in 5 volumes of 400 mmol/L NaCl. The tissue homogenate was titrated to pH 8.0 with 1 mol/L NaOH, allowed to stabilize, and then back titrated to pH 6.5 with standardized 0.1 mol/L HCl under a nitrogen atmosphere at 12 °C. The slope of the curve relating mmol HCl added to pH over the range 7.5–7.0 (the operative pHi range *in vivo* – *cf.* fig. 4A) was taken as the buffer capacity of the tissue in mmol/pH unit/kg. This was then converted to mmol/pH unit/L ICF water (slykes) taking into account the water content of the powdered tissue, its original water content, the appropriate ECFV (from table 4 for tissues; 30 ml/kg for the red cell pellet), and the β_{NB} of separated plasma (from Graham *et al.*, 1990) as an estimate of ECFV β_{NB}.

Analytical techniques. Analytical and statistical methods were identical to those described by Graham *et al.* (1990), with the following additions. CSF P_{CO_2} was calculated from the Henderson–Hasselbalch equation (as for EDF P_{CO_2}), based on measured pH and C_{CO_2} levels (15–25 μl normally analyzed) and apparent pK values for the CO_2/HCO_3^- equilibrium (pKapp) derived from the empirical relationship established for skate fluids by Graham *et al.* (1990). Tissue water contents were determined by drying to a constant weight at 65 °C; plasma, EDF and CSF water contents were calculated from the protein content determined by refractometry. Levels of ^{14}C- and ^{3}H-radioactivity in plasma, EDF, brain, heart, and muscle were determined by digesting duplicate 100 μl or 100–300 mg samples in 2 ml NCS tissue solubilizer (Amersham). Single CSF samples (5–50 μl, when available) were treated similarly. Once a clear solution was obtained, the digests were neutralized with glacial acetic acid, 10 ml of fluor (OCS; Amersham) were added, and the samples stored in the dark overnight to reduce chemiluminescence, prior to counting on an LKB Wallac 1217 liquid scintillation counter. Dual-label quench correction was performed using quench standards prepared from each type of tissue and the external standard ratio method (Milligan and Wood, 1986).

Results

Fluid and tissue buffer capacities. The non-HCO_3^- buffer capacities (β_{NB}) of CSF, EDF, and separated plasma were linearly related to their protein concentration (fig. 1). Protein concentrations measured in CSF were significantly lower than those in EDF which in turn were significantly lower than those in plasma (table 1). Thus, the mean β_{NB} estimated for CSF by this relationship was only about 60% of that for EDF, 25% of that for separated plasma, and 13% of that for whole blood.

Of the various tissues surveyed, brain had the lowest intracellular β_{NB} value, followed by heart ventricle, corresponding to approximately 50% and 70%, respectively, of the β_{NB} for white muscle (table 2). Red blood cells exhibited by far the highest buffer

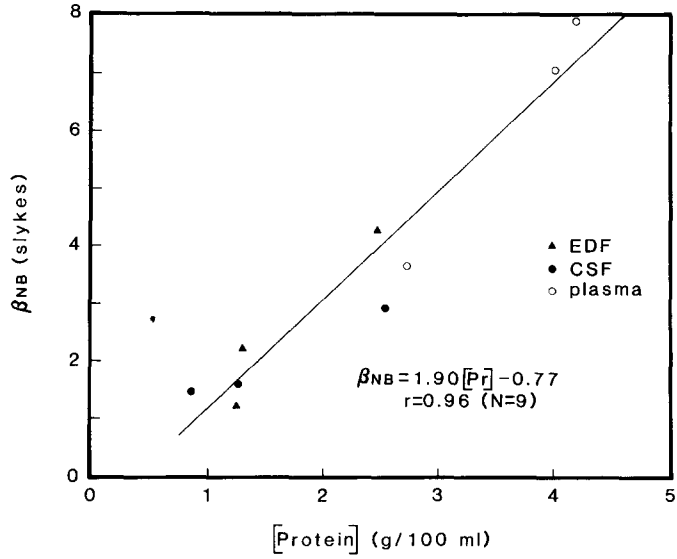

Fig. 1. The *in vitro* relationship at 12 °C in *R. ocellata* between protein concentration and the non-HCO_3^- buffer capacity (β_{NB}) of extradural fluid (EDF), cerebrospinal fluid (CSF), and separated blood plasma. Plasma and EDF (by catheter) and CSF (by terminal puncture) were sampled from 3 skate; each point represents a sample from one animal. The linear regression relationship ($P \leq 0.01$) is given.

capacity, 71 slykes on an intracellular water basis, as measured directly by acid titration (table 2).

Extracellular responses to hypercapnia. The magnitude and time course of changes in Pa_{CO_2}, pHa, and plasma HCO_3^- during exposure to PI_{CO_2} = 7.5 Torr, as determined by single terminal samples (fig. 2), were very similar to those recorded by serial sampling in the preceding study (Graham *et al.*, 1990). Notably, the normal Pa_{CO_2}–PI_{CO_2} gradient

TABLE 1

Protein concentration and estimated non-HCO_3^- buffer capacities (β_{NB}) of cerebrospinal fluid (CSF), extradural fluid (EDF), and separated blood plasma in the big skate at 12 °C. Means ± 1 SEM (*N*).

	Protein (g/100 ml)	β_{NB} [a] (slykes)
CSF	1.21 ± 0.08 (27)	1.53
EDF	1.80 ± 0.08 (37)	2.65
Plasma	3.86 ± 0.14 (48)	6.56
Whole blood [b]	–	11.04

[a] Estimated from protein concentration using the regression equation of fig. 1.
[b] From Graham *et al.* (1990).

TABLE 2

Intracellular buffer capacities (β_{NB}) of several tissues in the big skate at 12 °C. Means ± 1 SEM (N).

Tissue	β_{NB} [a] (slykes)
Brain	21.62 ± 2.42 (6)
Heart ventricle	29.33 ± 0.51 (5)
White muscle	40.57 ± 3.08 (5)
Red blood cells	70.75 ± 2.75 (5)

[a] Expressed per unit intracellular water.

of 0.5 Torr again more than doubled during hypercapnia, and the initial acidosis (0.5 units), rate of HCO_3^- build-up, and extent of compensation by 24 h (65%) were virtually identical. Changes in EDF acid–base status (not shown) were also identical to those measured by Graham *et al.* (1990), confirming that the slow pattern of response in the extradural compartment was not an artifact of serial sampling and saline replacement. Plasma and EDF ions (not shown) were also measured at every sample time, and in general confirmed the patterns of the previous study. The one exception was a significant increase in EDF Na^+ and Cl^- concentrations at 8–10 h, a time not analyzed for these parameters by Graham *et al.* (1990).

Under control conditions, CSF pH was approximately 0.2 pH units below the pHa of arterial blood (fig. 2B), and 0.1 units below EDF pH, reflecting a much higher P_{CO_2} (CSF = 2.7, EDF = 1.6, arterial blood = 0.8 Torr). However, in contrast to EDF, CSF P_{CO_2} rose in concert with Pa_{CO_2} during hypercapnia, and remained in equilibrium throughout the entire exposure (0.5–24 h; fig. 2A). Thus, blood-borne CO_2 rapidly equilibrated into this central fluid compartment of the brain. Despite the very low β_{NB} value of CSF relative to blood (table 1), its pH fell to a lesser extent (0.3 *vs* 0.5 units; fig. 2B). Even more remarkable was its rate of recovery during maintained hypercapnia. Indeed, CSF pH had returned to the control level by 8–10 h, a time at which pHa compensation was less than 50% (fig. 2B). This reflected a faster accumulation of HCO_3^- in the CSF (fig. 2C), together with a lower control pH value. There was no further change in CSF pH at 20–24 h.

As an independent check on the accuracy of the CSF pH measurements, CSF pH was also estimated from the measured distribution of ^{14}C-DMO dpm between plasma and CSF, and the measured pHa value. In other words, the CSF was treated as a tissue sample. Only samples where at least 15 μl were available for counting were included in this analysis. Most values agreed within 0.1 pH units by the two techniques, though in several cases the discrepancy was up to 0.25 units (fig. 3). Overall, there was a highly significant, almost 1 : 1 correlation between the two estimates of CSF pH, supporting the accuracy of the directly measured values (fig. 3). Thus, the weak organic acid DMO freely penetrated into this central fluid compartment of the brain, and distributed between plasma and CSF according to the pH gradient.

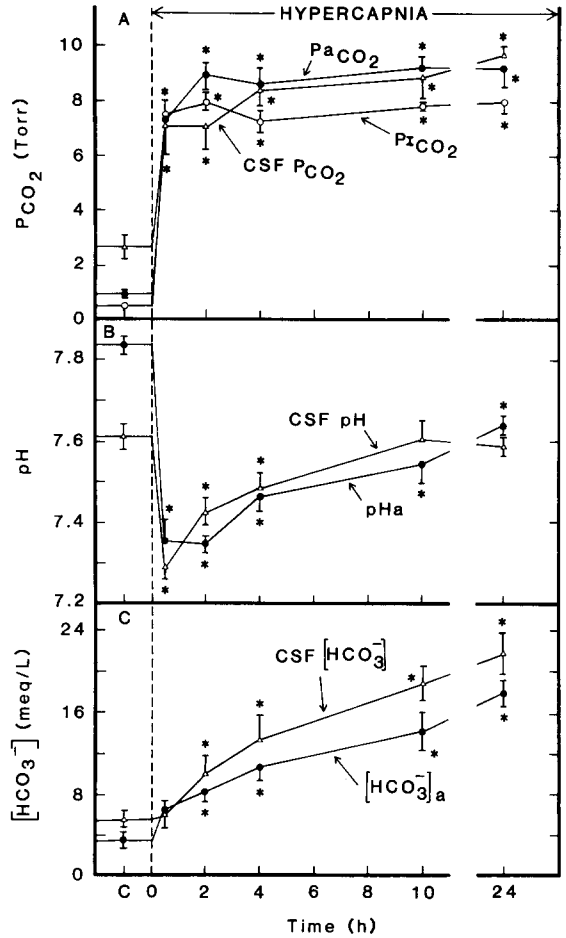

Fig. 2. The effects in *R. ocellata* of exposure to normoxic hypercapnia at 12 °C on (A) inspired (PI_{CO_2}), arterial (Pa_{CO_2}), and cerebrospinal fluid (CSF P_{CO_2}) CO_2 tensions; (B) arterial plasma (pHa) and CSF pH; and (C) arterial plasma ($[HCO_3^-]a$) and CSF bicarbonate concentrations. The normocapnic control measurement (at PI_{CO_2} = 0.3 Torr, PI_{O_2} = 155 Torr) is designated as C. Exposure to hypercapnia (PI_{CO_2} = 7.5 Torr, PI_{O_2} = 155 Torr) was instituted at time 0; all experimental times are exact, except the 10 h point which was sampled at 8–10 h, and the 24 h point which was sampled at 20–24 h. Each animal was sampled only once, terminally. Values are means ± 1 SEM; C (N = 9), 0.5 h (N = 5), 2 h (N = 6), 4 h (N = 6), 8–10 h (N = 5), and 20–24 h (N = 9). Asterisks indicate experimental means significantly different ($P \leq 0.05$) from normocapnic control.

In marked contrast to this equilibration of ^{14}C-DMO, the extracellular fluid marker ^{3}H-mannitol, a polar non-electrolyte, penetrated very poorly into the CSF, averaging only 26% of plasma levels at the time of sacrifice, 10–12 h after injection (table 3). The behaviour of these two markers in the EDF was very different from that in the CSF. Both mannitol and DMO in the EDF had reached approximately 70% of their respective plasma levels by 12 h (table 3), and there was no significant difference in their

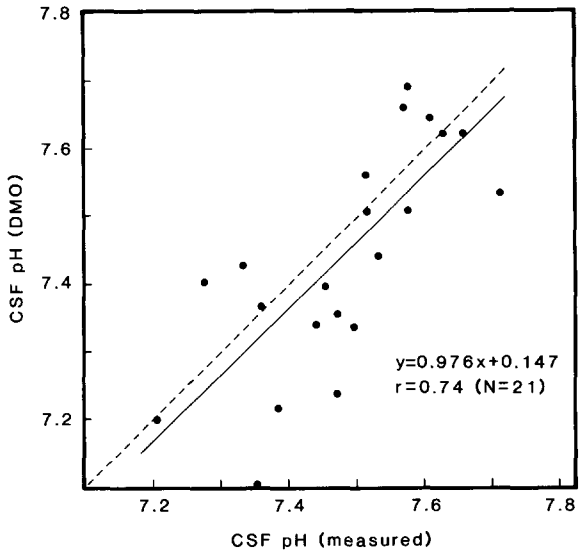

Fig. 3. The relationship in *R. ocellata* at 12 °C between directly measured cerebrospinal fluid (CSF) pH (X) and CSF pH as estimated from the measured distribution of ^{14}C-DMO between plasma and CSF (Y). Each point represents a terminal sample from one skate; points from animals at all different times during the experimental exposure are included. The solid line represents the regression relationship ($P \leq 0.001$); the dashed line represents the line of equality (Y = X).

distribution ratios (paired *t*-test), supporting the previous interpretation that EDF is formed very slowly from the blood plasma (Graham *et al.*, 1990). Given this situation, calculation of EDF pH from DMO distribution was clearly meaningless.

Intracellular responses to hypercapnia. Under control conditions, pHi values, as measured by DMO distribution, were highest (and not significantly different from one

TABLE 3

Distribution ratios of ^{3}H-mannitol and ^{14}C-DMO between cerebrospinal fluid (CSF) and blood plasma, and between extradural fluid (EDF) and blood plasma in the big skate at 12 °C, measured 10–12 h after injection. Means ± 1 SEM (*N*).

	^{3}H-mannitol (brain fluid/plasma)	^{14}C-DMO (brain fluid/plasma)
EDF	0.693 ± 0.026 (35)	0.771 ± 0.027 (35)
CSF	0.262 ± 0.023[a] (29)	0.983 ± 0.034[a,b] (29)

[a] Significantly different ($P \leq 0.05$) from corresponding EDF value.
[b] Significantly different ($P \leq 0.05$) from corresponding ^{3}H-mannitol value

another) in heart ventricle and brain, significantly lower in white muscle, and lowest in red blood cells (table 4). Upon exposure to hypercapnia, all four tissues were rapidly acidified (0.5 h), but the same pattern was maintained (fig. 4A). The two poorly buffered tissues, brain and heart (table 2) underwent smaller depressions in pHi ($\sim$0.3 units) than the two well buffered tissues, white muscle and red blood cells ($\sim$0.4 units). Furthermore, the initial rates of pHi correction in brain and heart were greater than in white muscle or red cells (fig. 4A). However, in marked contrast to the perfect regulation of CSF pH by 8–10 h (fig. 2B), brain pHi correction slowed considerably after 4 h (fig. 4A). An intracellular acidosis of $\sim$0.1 unit persisted in brain tissue at 20–24 h; thus, pHi correction was only 70% complete. A very similar pattern was seen in heart ventricle. The slow recovery of muscle and RBC pHi continued throughout the experiment, such that these tissues also achieved about 70% correction by 20–24 h (fig. 4A). This pattern of RBC pHi regulation during hypercapnia, together with unaltered or

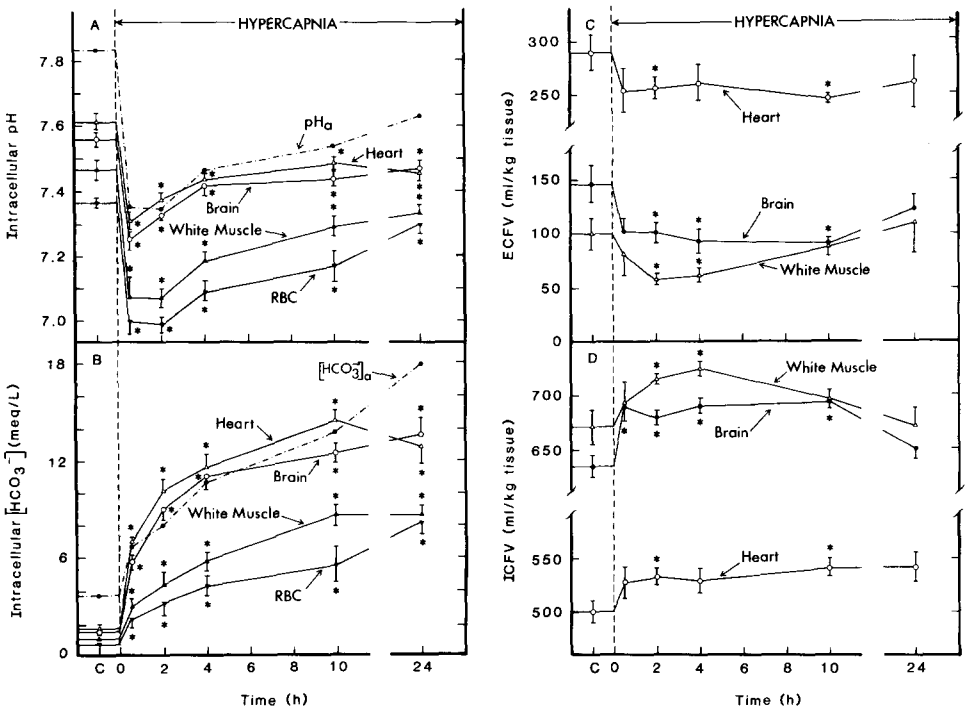

Fig. 4. The effects of exposure to normoxic hypercapnia on intracellular acid–base status and fluid volume distribution in *R. ocellata*. (A) Intracellular pH in heart ventricle, brain, white muscle, and red blood cells; and (B) bicarbonate levels in these same tissues, calculated on the assumption of equilibration of P_{CO_2} between arterial blood plasma and the intracellular compartments. Mean arterial blood plasma pH (pHa) and bicarbonate ($[HCO_3^-]a$) levels are indicated by the dotted lines. (C) Extracellular fluid volume (ECFV) in heart ventricle, brain, and white muscle; and (D) intracellular fluid volume (ICFV) in these same tissues. Total tissue water content in each tissue remained unchanged throughout the exposure at the levels shown in table 4. See legend of fig. 2 for other details.

TABLE 4

Intracellular pH values and fluid volume distributions in several tissues of the big skate under control normocapnic conditions at 12 °C. Means ± 1 SEM (*N*).

	pHi[a]	Water content (ml/kg)	ECFV (ml/kg)	ICFV (ml/kg)
Heart ventricle ($N = 8$)	7.62 ± 0.02	790.0 ± 3.2	289.5 ± 18.8	500.5 ± 11.0
Brain ($N = 8$)	7.56 ± 0.03	780.0 ± 9.0	146.2 ± 18.2	634.0 ± 13.5
White muscle ($N = 8$)	7.47 ± 0.03	772.9 ± 5.5	102.0 ± 16.7	670.9 ± 11.1
Red blood cells ($N = 8$)	7.36 ± 0.02	699.6 ± 14.5[b]	–	–

[a] At pHa = 7.84 ± 0.02 (8).

[b] Water content of red cell pellet after aspiration of plasma; trapped ECFV in pellet = 30 ml/kg.

slightly increased MCHC (mean cell hemoglobin concentration; not shown) and unchanged NTP/Hb (not shown), was identical to that monitored by serial sampling in the previous study (Graham *et al.*, 1990).

In fig. 4B, intracellular HCO_3^- changes have been calculated for individual tissues, assuming that the measured Pa_{CO_2} value in each fish was representative of the intracellular level. This analysis illustrates a marked difference in the pattern of HCO_3^- accumulation between brain and heart on the one hand, and muscle and red cells on the other. During most of the recovery period, intracellular HCO_3^- concentrations in brain and heart remained similar to those of arterial blood plasma, while muscle and RBC HCO_3^- were much lower.

Tissue water contents in brain, heart, and white muscle (control values in table 4) remained unchanged throughout hypercapnia, but the internal distribution of fluid between intra- and extra-cellular compartments shifted considerably (fig. 4C,D). In all three tissues, there was a net movement of water out of the ECFV into the ICFV during hypercapnia – *i.e.* a net swelling of the cells. This shift was greatest in the brain, where it was significant at all sample times during the first 10 h, and least in the heart, where it was significant at only two of the times. By 20–24 h, the distribution had re-established ECFV and ICFV levels not significantly different from control in all three tissues. ICFV was not measured directly in red blood cells. However, MCHC (not shown), which provides an inverse index of RBC swelling, showed no significant change. This supports the conclusion of Graham *et al.* (1990) that skate RBCs do not swell during hypercapnia, in contrast to those of other species, and other tissues of the skate itself (fig. 4C,D).

Discussion

Fluid and tissue buffer capacities. To our knowledge, the present measurements of β_{NB} in EDF and CSF (fig. 1, table 1) are the first such determinations in fish, though

previous studies have noted low protein concentrations (*cf.* table 1) for these fluids in other elasmobranchs (Zubrod and Rall, 1959; Cserr *et al.*, 1978). The protein concentrations measured in the CSF of *R. ocellata*, while less than one third of those of plasma levels, were somewhat higher than levels reported in various shark species, while EDF levels were comparable. It is not surprising that CSF, EDF, and separated plasma β_{NB} values all followed a common relationship with protein concentration (fig. 1), for according to Zubrod and Rall (1959) the proteins of the various compartments are electrophoretically indistinguishable. An important consequence of the very low β_{NB} in CSF is that it will tend to maximize pH changes (*i.e.* minimize passive buffering) when CSF P_{CO_2} changes. The observation that CSF pH was already significantly above that predicted for passive buffering by 0.5 h of hypercapnia (fig. 5B, discussed below), is testimony to the efficiency of active CSF acid–base regulation.

The present tissue β_{NB} determinations in skate (table 2) were obtained by titration of tissue homogenates. Recently, Wiseman and Ellington (1989) have reported that in muscle of the invertebrate *Busycon canaliculatum*, the homogenate technique yields significantly higher β_{NB} values than *in situ* methods using weak acid or base loading of whole tissue. At present, the exact meaning of this difference, and whether it applies to vertebrate tissue, are unclear. Nevertheless, the possibility that the titration method may overestimate tissue β_{NB} should not be overlooked.

The present results (table 2) showing brain, followed by heart ventricle, to have the lowest buffer capacities were in close quantitative agreement with those of Milligan and Wood (1986) on the rainbow trout (*Salmo gairdneri*). In contrast, white muscle β_{NB} was only about half the trout value. However, there appears to be considerable variation between species, probably related to the total amount of histidine-related compounds present. The skate muscle value was only slightly lower than that measured in the larger-spotted dogfish (*Scyliorhinus stellaris*; Heisler and Neumann, 1980). We are aware of no previous direct measurements of β_{NB} in red blood cells of fish using comparable methodology (*i.e.* acid titration of erythrocytes); it is more usual to titrate the whole blood with CO_2. However, it is reassuring that the directly measured value (71 slykes; table 2) agreed favourably with a value of 63 slykes calculated from the CO_2 titrations of whole blood in the same species (Graham *et al.*, 1990). Such a high buffer capacity is to be expected, given the high hemoglobin concentration of red blood cells. *A priori*, one might also expect that the greater the β_{NB} value of a tissue, the less would be its pHi depression during hypercapnia. However, this was clearly not the case in the present study (fig. 4A), for reasons outlined below.

Marker penetration into brain fluids. The differential entry of ^{14}C-DMO and ^{3}H-mannitol into the CSF of the skate (table 2) is in agreement with previous studies on both other elasmobranchs and mammals, and supports the interpretation that the permeability characteristics of the blood–brain barrier are similar in the two classes (Zubrod and Rall, 1959; Fenstermacher and Patlak, 1977; Cserr *et al.*, 1978; Cserr and Bundgaard, 1984). Polar non-electrolytes such as mannitol are effectively restricted by this functional barrier, but weak organic acids such as DMO freely penetrate. Therefore,

it is not surprising that DMO estimates of CSF pH agreed well with direct measurements (fig. 3), though we are aware of no previous studies in lower vertebrates which have reported this validation. The slower, non-specific entry of mannitol and DMO into the EDF is also in accord with earlier investigations, and supports the view that EDF is simply a slowly formed, slowly exchanging exudate of the blood plasma (Fenstermacher and Patlak, 1977).

CSF acid–base responses to hypercapnia. Qualitatively, the present observations on CSF acid–base status of the skate during hypercapnia confirm the original findings of Maren (1962a,b; 1972) on the spiny dogfish (*Squalus acanthias*). CSF P_{CO_2} rapidly equilibrated with Pa_{CO_2} during environmental hypercapnia (fig. 2A), indicating free penetration of CO_2 through the blood–brain barrier. The resultant fall in CSF pH was much smaller than that in pHa (fig. 2B), and was completely compensated within 8–10 h by a rapid accumulation of HCO_3^- (fig. 2C). H^+ and HCO_3^- clearly did not equilibrate across the blood–brain barrier, for pHa was still significantly depressed at 24 h, and plasma HCO_3^- levels remained lower than CSF levels. As in many mammalian studies (reviewed by Maren, 1972 and Schlaefke *et al.*, 1983), CSF pH regulation was more rapid and precise than blood pH regulation in both skate and dogfish, underlining the critical importance of the acid–base status of the fluid bathing the central nervous system. Through inhibition studies, Maren (1962b, 1972) demonstrated that carbonic anhydrase in the choroid plexus played an important role in the rapid HCO_3^- 'transport' process responsible for CSF pH control. Nevertheless, CSF pH regulation still occurred, albeit at a slower rate, when carbonic anhydrase was pharmacologically blocked. Essentially nothing else is known about the mechanism of CSF pH correction in fish, though analogy to higher vertebrates would suggest the involvement of a Cl^-/HCO_3^- exchange process (see papers in Schlaefke *et al.*, 1983).

Quantitatively, the present data on *R. ocellata* exhibited some differences from those of Maren (1962a,b; 1972) on the dogfish. In the skate under control conditions, CSF P_{CO_2} was higher, and CSF pH lower than the corresponding values in arterial blood (fig. 2A,B), in agreement with measurements in mammals. The opposite situation in the dogfish probably resulted from the traumatic blood sampling technique employed. In the dogfish, CSF pH depression during hypercapnia was smaller and more quickly corrected than in the skate. To a certain extent, this may have reflected differences in the exposure regime to hypercapnia; nevertheless, the rate of CSF HCO_3^- accumulation was clearly lower in the skate than in the dogfish. This may be related to the overall slower rate of systemic acid–base adjustment in the skate (Graham *et al.*, 1990) relative to sharks (Heisler, 1989). Maren (1972) also suggested that CSF pH might provide the proximate chemical control of respiration in the dogfish, though he made no measurements of ventilation. As outlined in detail below, the present data on the skate, in combination with the accompanying $\dot{V}w$ measurements of Graham *et al.* (1990), do not support this interpretation.

Comparison of the CSF acid–base responses with blood plasma responses by means of pH-HCO_3^- diagrams (fig. 5A,B), each with its appropriate non-HCO_3^- buffer line,

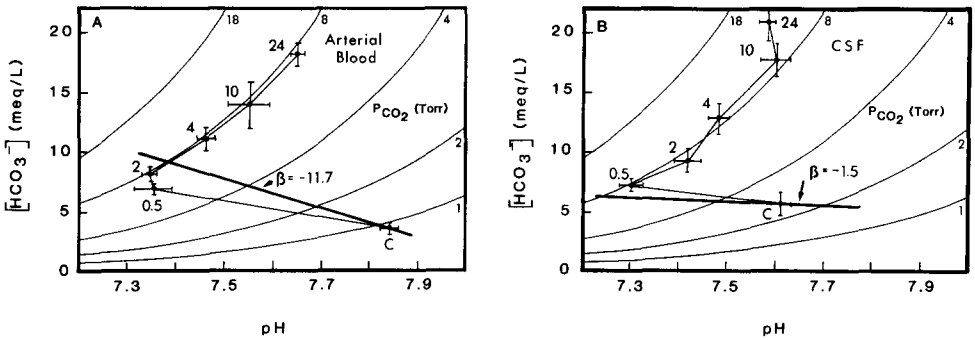

Fig. 5. A graphical representation in *R. ocellata* of the simultaneous changes in pH, HCO_3^-, and P_{CO_2} levels in (A) arterial blood plasma; and (B) cerebrospinal fluid (CSF) during 24 h exposure to normoxic hypercapnia. In (A), the non-HCO_3^- buffer relationship (heavy line) was plotted using the β_{NB} value appropriate for the mean measured hemoglobin concentration of these skate (from fig. 1B of Graham *et al.*, 1990); in (B), the relationship was plotted using the β_{NB} value appropriate for the mean measured CSF protein concentration of these skate (from fig. 1). Means ± 1 SEM. See legend of fig. 2 for other details.

emphasises the marked differences in regulation between the two compartments. In agreement with the results obtained by serial blood sampling in the preceding study (*cf.* fig. 4A of Graham *et al.*, 1990), plasma HCO_3^- accumulation during the first 2 h of hypercapnia was less than predicted by passive non-HCO_3^- buffering (fig. 5A). In contrast, by 0.5 h, CSF HCO_3^- accumulation was already accelerated above the point predicted by passive buffering (fig. 5B), evidence of the rapidity of the active regulation process.

Intracellular acid-base responses to hypercapnia. The intracellular acid–base responses of the four tissues studied (from fig. 4) are portrayed on pH-HCO_3^- diagrams in fig. 6, with appropriate β_{NB} values taken from table 2. This analysis emphasises the marked difference in behaviour between the brain, the tissue of principal interest in the present investigation, and the other three. Only the brain, the most poorly buffered of the four tissues (table 2), followed its passive non-HCO_3^- buffer line during the initial stages of hypercapnia (fig. 6A); the others all exhibited a compounding 'metabolic' acidosis of varying magnitude at this time (fig. 6B,C,D). Thereafter, there was a rapid active HCO_3^- accumulation in the brain. To a certain extent, this pattern of preferential brain pHi regulation was similar to the preferential CSF pH regulation (fig. 5), underlining the primacy of central acid–base regulation. However, in contrast to CSF, the build-up of HCO_3^- in the brain slowed considerably after 4 h, leaving pHi correction incomplete; a significant intracellular acidosis persisted at 20–24 h. When considered in combination with the $\dot{V}w$ measurements of Graham *et al.* (1990), this pattern suggests that brain pHi may play a significant role in ventilatory control (discussed below).

The initial loss of HCO_3^- equivalents (figs. 5, 6) from all compartments except CSF and brain during the first 0.5 h of hypercapnia, relative to the levels which should have been created by passive non-HCO_3^- buffering, was surprising. The possibility noted

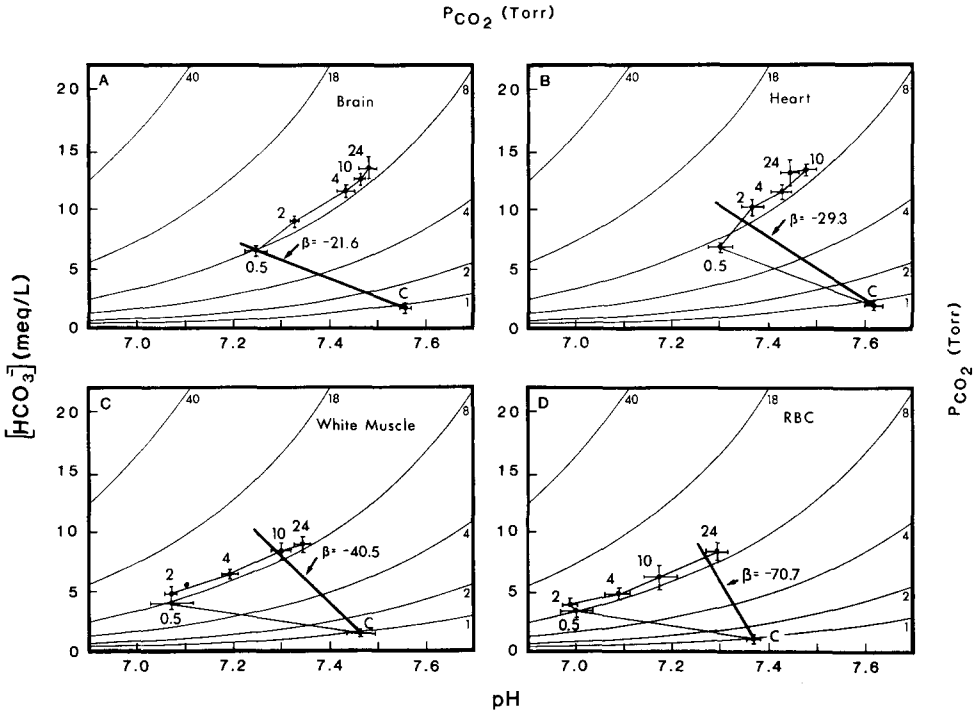

Fig. 6. Graphical representations in *R. ocellata* of the simultaneous changes in pH, HCO_3^-, and P_{CO_2} levels in the intracellular compartments of (A) brain; (B) heart ventricle; (C) white muscle; and (D) red blood cells, calculated on the assumption of equilibration of P_{CO_2} between arterial blood plasma and the intracellular compartments. In each case, the non-HCO_3^- buffer relationship (heavy line) was plotted using the appropriate measured value from table 2. Means ± 1 SEM. See legend of fig. 2 for other details.

earlier that the tissue β_{NB} values were significantly overestimated by the homogenate titration method (Wiseman and Ellington, 1989), and therefore that the HCO_3^- loss was apparent rather than real, cannot be eliminated. However, it is noteworthy that the greatest 'deficit' occurred in the most highly buffered intracellular compartment, the red blood cells, where homogenate titration and whole cell tonometry with CO_2 had yielded similar β_{NB} values. RBC acid–base status predicted from passive buffering was not regained until 24 h (fig. 6D). In the absence of active RBC pHi regulation in skate (discussed by Graham *et al.*, 1990) HCO_3^- was probably lost to the plasma, and only regained as plasma acid–base status was compensated. White muscle followed a similar trend, with compensation finally surpassing the point of passive buffering by 10 h (fig. 6C). Less well buffered heart ventricle underwent a much smaller initial loss (fig. 6B), and the weakly buffered brain tissue none at all (fig. 6A). Thus, substantial heterogeneity exists between compartments and passive buffering alone does not predict the response of an individual compartment in the intact animal.

Several possible explanations for the large initial deficit of HCO_3^- equivalents may be considered. Firstly, there may have been an initial transfer of HCO_3^- to other

(unmeasured) compartments in which pH was preferentially regulated. Obviously, the CSF was one such compartment (fig. 5B), but quantitatively could account for only a small fraction of the 'missing' HCO_3^-. Given the size of the white muscle mass, and the magnitude of its initial deficit, it seems most unlikely that this could be the complete explanation. Secondly, there could have been a initial loss of HCO_3^- equivalents to the environmental water across the gills. Fluxes to the environment were not measured in the present study. However, *Scyliorhinus stellaris* showed such a loss during the first 15 min of exposure to hypercapnia (reviewed by Heisler, 1989). Heisler's model calculations suggest that HCO_3^- was lost from ICF to ECF and from ECF to environment at this time, but the deficit was small relative to that in *R. ocellata*. The larger loss in the skate could well be the explanation for the overall slower rate of pH compensation in the skate relative to the dogfish. Thirdly, it remains possible that hypercapnia induced the production of unknown metabolic acid(s) in the tissues. Further work is needed to separate these possibilities and clarify their possible adaptive significance.

The progressive accumulation of HCO_3^- equivalents in all compartments after 0.5 h was probably due to uptake from the water into the ECF (or acidic equivalent excretion into the water) followed by redistribution into the ICF, as documented in the dogfish (reviewed by Heisler, 1989). Notably, the brain and heart ventricle, which might be considered 'essential' tissues, increased their HCO_3^- to the same levels as those of blood plasma (fig. 4B). This resulted in a more rapid pHi adjustment during the early hours of hypercapnia than in white muscle or red blood cells. However, the latter tissues continued to accumulate HCO_3^- throughout hypercapnia, whereas the process slowed considerably after 4 h in brain and heart. By 24 h all tissues had developed about the same extent of pHi correction ($\sim 70\%$), but the pH-HCO_3^- diagrams illustrate that this simple percentage figure is misleading because the correction was achieved in different ways by the various tissues (fig. 6). To cite the two extremes, in brain, this result reflected active HCO_3^- accumulation against a background of low passive buffering and no initial HCO_3^- deficit (fig. 6A), while in red blood cells it reflected a return to the status provided by passive buffering alone against a background of almost complete initial loss of the HCO_3^- generated passively (fig. 6D).

We are aware of no previous time course studies on regional pHi correction during environmental hypercapnia in fish. Instead, measurements have been made either immediately (Wright *et al.*, 1988) or after 1–5 days (Cameron, 1985; Heisler, 1989); the latter indicated comparable inter-tissue heterogeneity to that of the present study. However, the time course of regional pHi recovery over the 12 h period following exhaustive exercise has been documented in two teleosts (Milligan and Wood, 1986, 1987). These data were in agreement in showing more rapid pHi correction in brain and heart than in white muscle, though the teleosts also exhibited efficient RBC pHi regulation, in contrast to the skate.

A shift of fluid into red blood cells during hypercapnia has been documented in a variety of fish, and attributed to both a passive Donnan effect and active RBC pHi regulation (see Graham *et al.*, 1990). In *R. ocellata*, red cell swelling could not be detected, perhaps at least partially due to the absence of RBC pHi regulation. Curiously

however, there was marked fluid shift from ECFV to ICFV in brain, white muscle, and heart (fig. 4C,D). This effect does not appear to have been noted in previous studies on environmental hypercapnia in fish. However, Heisler (1982) reported a significant reduction of whole body ECFV when the air-breathing teleost *Synbranchus marmoratus* experienced self-induced hypercapnia accompanying the switch from aquatic to aerial respiration. There was also a shift of fluid from ECFV to ICFV in the white muscle of rainbow trout during self-induced hypercapnia caused by exposure to hyperoxia (C. M. Wood, unpublished data). In all these cases, the explanation could be a simple Donnan effect associated with high CO_2, ionic shifts associated with pHi regulation, or the intracellular generation of osmotically active products, such as the unknown metabolic acid alluded to earlier. Further research is required before any firm conclusions can be drawn.

CSF and brain acid–base status and the control of ventilation. The primary objective of this study was to assess whether the acid–base status of the CSF, the brain tissue itself, or both would correlate with the ventilatory responses seen during hypercapnia. Fig. 7 relates the mean $\dot{V}w$ changes measured over 24 h of hypercapnic exposure, from Graham *et al.* (1990), to measured changes in each of pHa, CSF pH, brain pHi, and Pa_{CO_2}. This analysis re-inforces the conclusion of Graham *et al.* (1990) that ventilation was best correlated with pHa (fig. 7A).

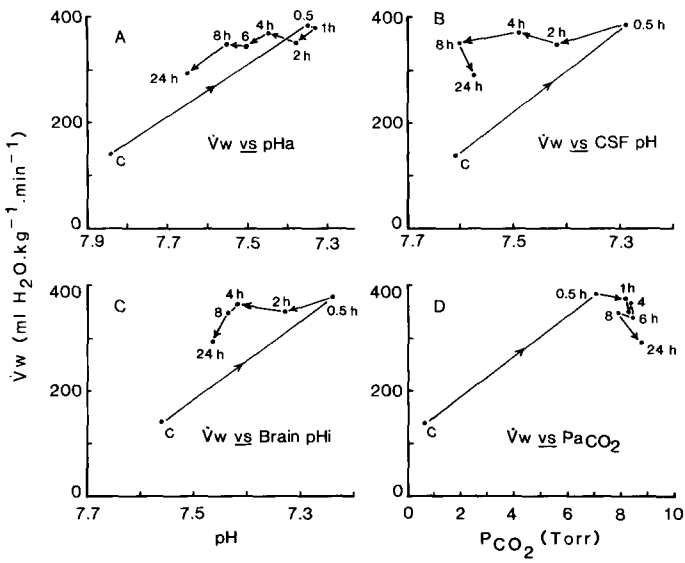

Fig. 7. Relationships between measured changes in ventilation ($\dot{V}w$; from fig. 2 of Graham *et al.*, 1990) and measured changes in (A) arterial pH (pHa); (B) cerebrospinal fluid pH; (C) brain intracellular pH; and (D) arterial CO_2 tension (Pa_{CO_2}) in *R. ocellata* during 24 h of exposure to normoxic hypercapnia. In (B) and (C) the 8–10 h and 20–24 h pH measurements are plotted at 8 h and 24 h respectively to coincide with the $\dot{V}w$ measurements at these times. Means only; see legend of fig. 2 for other details.

In contrast to the suggestion of Maren (1972) for the dogfish and the commonly assumed situation in higher vertebrates, $\dot{V}w$ did not appear to be keyed to CSF pH, at least on a long term basis. Elevated ventilation persisted long after CSF pH had been regulated back to control levels (fig. 7B). We cannot eliminate the possibility that acidosis in the CSF at the onset of hypercapnia contributed to the initiation of the ventilatory response. However, after 20–24 h, factors other than CSF pH were clearly responsible. A more promising candidate for central involvement in ventilatory stimulation was brain pHi (fig. 7C), for the persistence of intracellular acidosis in the brain at 20–24 h could explain the persistent elevation of ventilation. This situation does not necessarily differ from that in higher vertebrates, for it remains controversial whether CSF pH, medullary interstitial pH, medullary pHi, or some combination thereof is the important controlling factor (see papers in Schlaefke *et al.*, 1983; Cherniack *et al.*, 1988). Finally, a plot of $\dot{V}w$ *vs* CSF P_{CO_2} has been omitted because it would be virtually identical to fig. 7D in light of the rapid equilibrium between arterial blood and CSF P_{CO_2} (*cf.* fig. 2A). In any event, CSF or blood P_{CO_2} did not appear to be the proximate stimulus, because P_{CO_2} continued to rise gradually with time while $\dot{V}w$ declined.

In summary, we conclude that pHa and brain pHi are the two most likely candidates for proximate stimuli in the CO_2/pH effect on ventilation which we and Heisler *et al.* (1988) have now demonstrated in elasmobranchs. In the intact unanaesthetised animal, it is very difficult to manipulate one without changing the other, or simultaneously altering related systemic and central acid–base variables. Analyses such as the present are at best correlative. Future research on this topic might be profitably directed at applying acid–base stimuli directly to the brain and CSF in anaesthetised, brain-exposed preparations, and in attempting to locate and record from the putative pHa receptors on the arterial bloodstream.

Acknowledgements. The authors again thank Dr D.R. Idler, former Director of the Marine Sciences Research Laboratory, Memorial University of Newfoundland, and his staff for their hospitality and assistance, and particularly Dr G.L. Fletcher who provided many resources for this study. This research was supported by operating grants from NSERC to CMW.

References

Cameron, J.N. and G.A. Kormanik (1982). Intracellular and extracellular acid–base status as a function of temperature in the fresh water channel catfish, *Ictalurus punctatus*. *J. Exp. Biol.* 99: 127–142.

Cameron, J.N. (1985). The bone compartment in a teleost fish, *Ictalurus punctatus*: size, composition, and acid–base response to hypercapnia. *J. Exp. Biol.* 117: 307–318.

Cherniack, N.S., M.G. Altose and S.G. Kelsen (1988). Control of respiration. In: Physiology, 2nd ed., edited by R.M. Berne and M.N. Levy. St. Louis: C.V. Mosby, pp. 624–635.

Cserr, H.F., J.F. Fenstermacher and D.P. Rall (1978). Comparative aspects of brain barrier systems for nonelectrolytes. *Am. J. Physiol.* 234: R52–R60.

Cserr, H.F. and M. Bundgaard (1984). Blood–brain interfaces in vertebrates: a comparative approach. *Am. J. Physiol.* 246: R277–R288.

Fenstermacher, J.D. and C.S. Patlak (1977). CNS, CSF and extradural fluid uptake of various hydrophilic materials in the dogfish. *Am. J. Physiol.* 232: R45–R53.

Graham, M.S., J.D. Turner and C.M. Wood (1990). Control of ventilation in the hypercapnic skate, *Raja ocellata*. I. Blood and extradural fluid. *Respir. Physiol.* 80: 251–270.

Heisler, N., H. Weitz and A. Weitz (1976). Extracellular and intracellular pH with changes of temperature in the dogfish *Scyliorhinus stellaris*. *Respir. Physiol.* 26: 249–263.

Heisler, N. and P. Neumann (1980). The role of physico-chemical buffering and of bicarbonate transfer processes in intracellular pH regulation in response to changes of temperature in the larger spotted dogfish (*Scyliorhinus stellaris*). *J. Exp. Biol.* 85: 99–110.

Heisler, N. (1982). Intracellular and extracellular acid–base regulation in the tropical freshwater teleost fish *Synbranchus marmoratus* in response to the transition from waterbreathing to airbreathing. *J. Exp. Biol.* 99: 9–28.

Heisler, N., D.P. Toews and G.F. Holeton (1988). Regulation of ventilation and acid–base status in the elasmobranch *Scyliorhinus stellaris* during hyperoxia induced hypercapnia. *Respir. Physiol.* 71: 227–246.

Heisler, N. (1989). Acid-base regulation. In: Physiology of Elasmobranch Fishes, edited by T.J. Shuttleworth. Berlin: Springer-Verlag, pp. 215–252.

Maren, T.H. (1962a). Ionic composition of cerebrospinal fluid and aqueous humour of the dogfish, *Squalus acanthias*: I. Normal values. *Comp. Biochem. Physiol.* 5: 193–200.

Maren, T.H. (1962b). Ionic composition of cerebrospinal fluid and aqueous humour of the dogfish, *Squalus acanthias*: II. Carbonic anhydrase activity and inhibition. *Comp. Biochem. Physiol.* 5: 201–215.

Maren, T.H. (1972). Bicarbonate formation in cerebrospinal fluid: role in sodium transport and pH regulation. *Am. J. Physiol.* 222: 885–899.

Milligan, C.L. and C.M. Wood (1985). Intracellular pH transients in rainbow trout tissues measured by dimethadione distribution. *Am. J. Physiol.* 248: R668–673.

Milligan, C.L. and C.M. Wood (1986). Tissue intracellular acid–base status and the fate of lactate after exhaustive exercise in the rainbow trout. *J. Exp. Biol.* 123: 123–144.

Milligan, C.L. and C.M. Wood (1987). Muscle and liver intracellular acid-base and metabolite status after strenuous activity in the inactive, benthic starry flounder (*Platichthys stellatus*). *Physiol. Zool.* 60: 54–68.

O'Regan, R.G. and S. Majcherczyk (1982). Role of peripheral chemoreceptors and central chemosensitivity in the regulation of respiration and circulation. *J. Exp. Biol.* 100: 23–40.

Randall, D.J., N. Heisler and F. Drees (1976). Ventilatory response to hypercapnia in the larger spotted dogfish *Scyliorhinus stellaris*. *Am. J. Physiol.* 230: 590–594.

Schlaefke, M.E., H.P. Koepchen and W.R. See (Eds.) (1983). Central Neurone Environment and the Control Systems of Breathing and Circulation. Berlin, Springer-Verlag, 271 p.

Waddell, W.J. and T.C. Butler (1959). Calculation of intracellular pH from the distribution of 5,5-dimethyl-2,4-oxazolidine dione (DMO): application to skeletal muscle of the dog. *J. Clin. Invest.* 38: 720–729.

Weiskopf, R.B., V. Fencl and R.A. Gabel (1977). CSF pH and P_{CO_2} measurement. *J. Appl. Physiol.* 43: 566–567.

Wiseman, R.W. and W.R. Ellington (1989). Intracellular buffering capacity in molluscan muscle: superfused muscle *versus* homogenates. *Physiol. Zool.* 62: 541–558.

Wright, P.A., D.J. Randall and C.M. Wood (1988). The distribution of ammonia and H^+ between tissue compartments in lemon sole (*Parophrys vetulus*) at rest, during hypercapnia, and following exercise. *J. Exp. Biol.* 136: 149–175.

Zubrod, C.G. and D.P. Rall (1959). Distribution of drugs between blood and cerebrospinal fluid in the various vertebrate classes. *J. Pharmacol. Exp. Ther.* 125: 194–197.